

Influence of hot water extraction on cell wall and OSB strand mechanics

J. J. Paredes¹ · S. Shaler² · C. Howell³ · J. Jakes⁴

Received: 18 January 2016 / Published online: 12 September 2017
© The Author(s) 2017. This article is an open access publication

Abstract The exposure of wood to elevated temperatures during hot water extraction (HWE) has been shown to significantly influence a variety of physical and chemical properties of the wood. Aspen (*Populus tremuloides*) and hemlock (*Tsuga canadensis*) strands underwent HWE at 160 °C for four different periods of time. The weight loss (WL) associated with the processes ranged from 2.9 to 17.3% for the aspen, and from 2.9 to 12.8% for the hemlock. The higher WL associated with the hardwood was attributed to higher hemicellulose content in the hardwood than in the softwood as well as differences in chemical composition. Substantial increases in cell wall hardness (up to 34%) and modulus of elasticity (MOE) (up to 28%) were obtained at the intermediate extraction conditions. Extended exposure conditions resulted in decreases. The axial MOE of strands showed significant differences only in aspen. These changes are hypothesized to be related, in part, to changes in cellulose crystallinity.

✉ J. J. Paredes
juan.paredes@unah.edu.hn; jparedesheller@gmail.com

¹ Universidad Tecnológica Centroamericana (UNITEC), Tegucigalpa, Honduras

² School of Forest Resources, Advanced Structures and Composites Center, University of Maine, Orono, ME 04469-5755, USA

³ University of Harvard, Cambridge, MA 02138, USA

⁴ Forest Products Laboratory, USDA Forest Service, Madison, WI 53726, USA

Introduction

In earlier evaluations of the physical and mechanical properties of oriented strand board (OSB) produced from hot water-extracted red maple, it was found that a 17% weight loss (WL) resulted in significant reductions in internal bonding (IB), modulus of rupture (MOR), although the flexural modulus of elasticity (MOE) remained unchanged. When southern yellow pine (SYP) was extracted at a 9% WL, MOE showed a significant increase, while MOR and IB had a slightly significant decrease. Other studies where wood was treated at high temperature showed a slight increase in MOE for short extraction time resulting in 8% WL, but as the time was extended the MOE decreased (Rusche 1973; Hill 2006). The properties of OSB can be further manipulated, depending on the conditions under which the material is manufactured (Gardner et al. 1993).

Phenomena influence the mechanical properties of OSB at multiple scales including: the panel, strand, cell wall, and molecular (polymeric) levels. At the panel level, the mechanical properties of OSB are affected by a broad number of factors such as material properties (e.g., species), resin system, and manufacturing procedures. Each component complements and affects the others in so many complex ways that it is difficult to determine the effect of individual variables in isolation.

At the strand and wood cell wall level, however, mechanical performance can be isolated from the influence of OSB manufacturing variables somewhat simplifying analysis. Axial MOE determination using nanoindentation measurements can be used to understand the mechanical response. This research focused on determining the influence of WL on the mechanical properties of wood cell walls at the strand level, which may have contributed to the changes in the previously mentioned research.

Materials and methods

Hot water extraction

In OSB manufacture, soft and hardwood species are used. There is a difference in their chemical composition (Fengel and Wegener 1984) and wood properties. To provide a more complete understanding of the differences in strength between them, hemlock (*Tsuga canadensis*) and aspen (*Populus tremuloides*) were chosen. The hemlock and aspen trees used in this work had a 12.4 m height and 22.8 cm diameter and 13.3 m height and 21.6 cm diameter, respectively. Each tree was felled and trimmed into logs of 4 ft. long, then manually debarked and used to create 10.2 ± 0.2 cm strands with a target thickness of 0.81 ± 0.05 mm using a Carmanah 12/48 ring-strander. A counterknife angle of 70° was used at a ring speed of 638 rpm. The majority of fines were removed using an Acrowood Trillium and Diamond Roll combination screen. Strands were conditioned in a dehumidification

dry kiln, at 50 °C and a relative humidity (RH) of 80% for 6 days until constant weight was attained. The average MC of the strands was of $14.5 \pm 0.3\%$.

Hot water extraction (HWE) has been successfully used to remove sugar (hemicelluloses) from wood by several researchers (Sattler et al. 2008; Tunc and van Heiningen 2008). The strands were treated with a HWE process conducted at 160 °C and four extraction times. They were placed in 300 g batches (oven dry basis) inside a digester, previously filled with fresh water at a ratio of 6:1 (water/wood). This ratio included water from the moisture content (MC) of the wood itself. The vessel was heated from room temperature to 160 °C in 50 min (preheating time), followed by constant temperature exposure times of 0, 25, 45 or 90 min. These four extraction conditions were equated to a severity factor (SF) through the use of Eq. (1) (Overend and Chornet 1987; Mosier et al. 2002).

$$SF = \log \left(\int_0^t \text{Exp} \left[\frac{(T_r - T_b)}{14.75} \right] dt \right) \quad (1)$$

where t is the residence time (min), T_r is the reaction temperature (°C), and T_b is the base temperature at 100 °C. The temperature difference was 14.75 (°C) derived from $\frac{T_r - T_b \cdot R}{E_a}$, assuming that the overall process is hydrolytic and the overall conversion is pseudo-first order (Overend and Chornet 1987; Mosier et al. 2002). Bonds on SF equation are from 0 (unextracted wood) to 4. Using Eq. (1) a SF of 2.72, 3.38, 3.56 and 3.84 was calculated for 0, 25, 45 and 90 min extraction time, respectively. Strand weight loss (WL) as a result of the extraction process was determined for each extraction run by freeze drying the extracted liquid at -42 °C under a vacuum between 1.3 and 1.5 Pa for approximately 48 h. Extracted strands were not washed afterward.

After the extraction process, all strands were conditioned in an environmental chamber at 21 °C and a relative humidity (RH) of 65% for 15 days.

Nanoindentation procedure

Theory

With indents approximately 1 μm across, nanoindentation is well suited to probe the mechanical properties of the micron-sized domains in wood and has yielded numerous valuable results in wood science research over the past decade (Wimmer and Lucas 1997; Konnerth and Gindl 2006; Tze et al. 2007). In this investigation, nanoindentation was used to measure the effects of HWE on the longitudinal elastic modulus and hardness of S2 cell wall laminate (SCWL) of tracheids in hemlock and fiber cells in aspen. A nanoindentation experiment consists of pressing a carefully shaped diamond tip into a material to a prescribed load while continuously recording the depth and displacement. From a nanoindent, the Meyer's hardness (H) is defined as

$$H = \frac{P_0}{A} \quad (2)$$

where P_0 is the maximum load and A is the contact area of the nanoindent. The contact area can be calculated based on a contact depth and an indenter shape function (Oliver and Pharr 2004), or directly measured from an image of the residual indent impression after the indenter is removed (Jakes et al. 2008, 2009). In this work, it is relied upon A measured directly from images.

In the nanoindentation experiment, the elastic properties of the material are captured by the initial slope of the unloading portion of a load-depth trace that has been corrected for external compliances (explained below). The inverse of the initial unloading slope is the contact compliance, C_p , which is the compliance attributable to the specimen and indenter tip. The C_p is related to the effective modulus, E_{eff} , through

$$C_p = \frac{1}{E_{\text{eff}}A^{1/2}} \quad (3)$$

For indentation against a homogenous, isotropic, elastic half-space,

$$\frac{1}{E_{\text{eff}}} = \frac{1}{\beta} \left(\frac{1 - \nu_s^2}{E_s} + \frac{1 - \nu_d^2}{E_d} \right) \quad (4)$$

where E_s and E_d are Young's moduli and ν_s and ν_d are Poisson's ratios of specimen and indenter, respectively. β is a numerical factor, which is set equal to 1.23 (Jakes et al. 2008). To calculate E_s in this study, E_d and ν_d for the diamond tip were taken to be 1137 GPa and 0.07, respectively. The value of Poisson's ratio used for SCWL was assumed to be 0.45 (Wimmer et al. 1997).

The load-depth trace must be corrected for external compliances, namely the machine compliance, C_m , and structural compliance, C_s (Jakes et al. 2008, 2009), before the elastic modulus can be accurately determined. The C_m arises from displacements in the load frame of the nanoindenter and is a constant for every nanoindentation performed. Methods to measure C_m have previously been established. The C_s arises from heterophase interfaces near the nanoindents and specimen-scale flexing and can vary sensitively as a function of position within a specimen (Jakes et al. 2008, 2009). An indent placed in the SCWL is in close proximity to heterophase interfaces, such as the interface between the cell wall lamina and middle lamella or free edge between a cell wall lamina and empty lumen. In addition, wood is an open cellular structure which may flex when a single cell wall is loaded. Therefore, to accurately calculate the elastic modulus from nanoindentation experiment performed on the SCWL, the load-depth traces must be corrected for C_s using the methods of Jakes et al. (2008, 2009). The C_s and C_m behave similarly and the sum of these external compliances ($C_m + C_s$) can be determined at each indent location using SYS correlations constructed from the data from multiloading indents. The SYS correlation (Jakes et al. 2008, 2009) is given by

$$C_t P_{\text{max}}^{1/2} = (C_m + C_s) P_{\text{max}}^{1/2} + \frac{H^{1/5}}{E_{\text{eff}}} \quad (5)$$

where C_t is the total compliance from the uncorrected curve and E_{eff} is the effective modulus. If $H^{1/2}/E_{\text{eff}}$ and $C_m + C_s$ are independent of load, then $C_t P_0^{1/2}$ plotted as a

function of $P_0^{1/2}$ forms a straight line of slope $C_m + C_s$. $C_m + C_s$; it can then be used to correct the load-depth trace.

Specimen preparation

Transverse cross sections in the latewood of hemlock and aspen were prepared for nanoindentation experiments. Previous researchers (Wimmer and Lucas 1997; Konnerth and Gindl 2006; Tze et al. 2007) first embedded wood specimens in epoxy to aid in sectioning. However, it is uncertain if the epoxy embedment infiltrates the cell walls. In addition, it was observed that the size of pores in the cell walls of red maple (*Acer rubrum* L.) increased with SF in HWE strands, suggesting the effect of epoxy embedment could change with increasing SF, masking real changes to cell wall properties caused by HWE. To eliminate the possibility of any undesired modification caused by the epoxy, a specimen preparation method was used which did not use embedment. An approximately 7×3 mm (longer dimension corresponds to longitudinal direction) was cut from a strand with a hand razor and adhered to a steel slug using a fast cure adhesive (Fig. 1).

The adhesive did not penetrate the cells that were tested. The steel slug was fit into a sledge microtome fit with disposable microtome blades and a gently sloping apex ($\sim 15^\circ$) was created in the transverse cross section. The slug was then mounted in an ultramicrotome equipped with a diamond knife and the apex was cut off, revealing a surface approximately 0.5 mm^2 that was suitable for nanoindentation experiments.

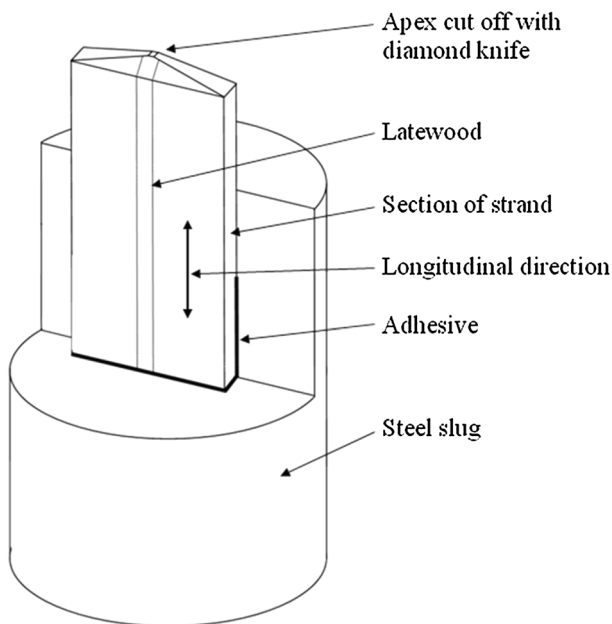


Fig. 1 Typical specimen preparation method for nanoindentation

Nanoindentation procedure

Nanoindentation experiments were performed with a Hysitron (Minneapolis, MN, USA) Triboindenter equipped with a Berkovich tip and operated in force control. The multiloading indent load function consisted of 1 s loading segments, 10 s holds at partial loads, 1 s unloading segments, and 5 s holds at partial unloads. There were seven loading segments loaded to loads of 15, 24, 35, 48, 63, 81, and 100% of the final maximum load. Each partial load was increased by approximately 50% of the final previous partial load, and the final partial unload was held for 60 s to calculate thermal drift before complete unloading.

Imaging indents and measuring areas

Residual indents were imaged with a Quesant (Agoura Hills, CA, USA) atomic force microscope (AFM) incorporated in the Triboindenter. The AFM was operated in contact mode and calibrated using an Advanced Surface Microscopy, Inc. (Indianapolis, IN, USA) calibration standard with a pitch of 292 ± 0.5 nm. Individual 4- μm field of view images (Fig. 2) were made of each indent, and ImageJ (<http://rsb.info.nih.gov/ij/>) image analysis software was used to manually measure the projected contact areas as described in previous publications (Jakes et al. 2008, 2009).

Axial elastic modulus of wood strands procedure

A small wood strand (beam) 28 mm long (22 mm span), 4.2 ± 0.3 mm wide was cut in the longitudinal direction (0° grain angle). Thickness was of 0.8 ± 0.1 mm for aspen and 0.7 ± 0.1 mm for hemlock. Earlywood and latewood were identified and measured, with an average earlywood portion approximately 92%, for both aspen and hemlock. All specimens were subjected to three-point bending using a Rheometrics Dynamic Mechanical Thermal Analysis (DMTA) instrument model

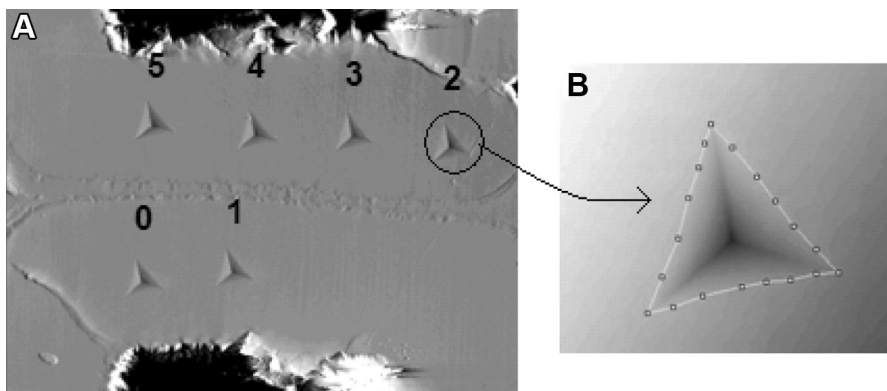


Fig. 2 AFM image taken after testing. **a** 2 μm scan of S2 wood cell wall layer, and **b** measured areas of each nanoindenter

IV. The test temperature was 21.7 ± 0.3 °C with a constant strain rate of 1.1×10^{-4} mm/s. This strain rate was obtained from a previous test. Immediately prior to testing, each sample was weighed using an Ohaus laboratory balance with precision of 1×10^{-4} g and measured using a Mitutoyo digital caliper with precision of 1×10^{-5} mm. As soon as flexural test was completed, the specimens were oven-dried at 103 °C for 24 h to determine the MC and density.

X-ray diffraction

Three strands were randomly selected from each species group and from the four SF and control conditions. Individual samples of $0.8 \times 25.4 \times 25.4$ mm³ were trimmed and scanned using a Panalytical X'Pert XRD machine. The $\theta - 2\theta$ diffraction scans were performed using a graded multi-layer parabolic X-ray mirror and 0.18° parallel plate collimator in quasi-parallel beam geometry. The step size was 0.1 mm with a total range of 5°–32°. Peaks were fitted to the scans using the program Profile Fit (Panalytical, the Netherlands, 1999, version 1.0C). The integrated areas of the fitted peaks were used to determine percent crystallinity according to previously described methods (Howell et al. 2009, 2011). Cross-sectional width of the crystalline regions was determined using the Scherrer formula

$$X_s = \frac{0.9\lambda}{B \cos \theta} \quad (6)$$

where X_s is the width (nm), λ the wavelength of the X-ray source, B the full width at half of the maximum of the peak (rad), and 2θ the angle between the source and the sample (rad). The Rietveld analysis method of analysis (Rietveld 1967, 1969) with the recently published crystalline structure of cellulose I β (Nishiyama et al. 2002) was also performed to verify the results using the program HighScore Plus (Panalytical, the Netherlands, 2006, version 2.2).

Results and discussion

Weight loss (WL) response was analyzed using Table 1. Results showed statistical differences in both SF and species (p value 0.0001). At the highest SF of 3.84 the highest WL occurred, 17.4 and 12.8%, for aspen and hemlock, respectively.

These results are consistent with other hardwood and softwood species (Hill 2006). There are two factors associated with the higher WL of hardwoods compared to softwoods: (1) Hardwoods are less thermally stable than softwoods. Ramiah and Goring (1967) studied the thermal degradation of isolated birch xylan and a spruce glucomannan, by determining the rate of gas evolution from the heated samples. These experiments showed that the hardwood xylan was less thermally stable than the softwood hemicelluloses, (2) The hemicellulosic content and composition in hardwoods have higher acetyl content than softwoods (Fengel and Wegener 1984). Rowell (2005) confirmed that aspen has a higher acetyl content than hemlock, 3.4 versus 1.7%, respectively. According to Tunc and van Heiningen (2008), the analysis of the liquid extract at 150 °C (hot water extraction) a mixture of southern

Table 1 Weight loss results of softwood (hemlock) and hardwood (aspen) from four different severity factors based on three replicas

Factors/levels	Count	Mean (%)	<i>p</i> value
<i>Aspen</i>			
2.72	3	2.92 ^a ± 0.14 ^A	0.0001
3.38	3	11.41 ± 0.74 ^B	
3.56	3	13.58 ± 0.85 ^C	
3.84	3	17.29 ± 0.36 ^D	
<i>Hemlock</i>			
2.72	3	2.94 ± 0.15 ^A	0.0001
3.38	3	7.76 ± 0.32 ^B	
3.56	3	10.14 ± 0.71 ^C	
3.84	3	12.81 ± 0.36 ^D	
<i>Main effects</i>			
A: SF	3	0.0001	
B: Species	1	0.0001	
<i>Interactions</i>			
AB	3	0.0001	

^a Mean value ± 2 standard deviations (95% confidence interval)

A,B,C,D Bonferroni multiple comparisons at the 95.0% confidence level

hardwoods showed that the pH decreased as the SF increased. This was consistent with the generation of acetic acid.

This acetyl content is the principal origin of acid formation when wood is soaked in water and is exposed to temperatures over 140 °C. These conditions cause cellular breakdown and production of condensable fractions, with significant loss of hemicelluloses, a small percent of lignin, constitution water and volatile extractives due to the production of organic acids, mostly acetic acid (Hill 2006; Tunc and van Heiningen 2008; Borrega and Karenlampi 2008).

In softwood species, the acetic groups contain galactoglucomannan, comprising 5–10% of its oven dry weight, with an average of one acetyl group for every four backbone units (Sjöström 1993). While in hardwoods, acetic acid comes from xylans, around 20–30% of its oven dry weight, contains an average of seven acetyl groups for every 10 xylose units.

Tunc and van Heiningen (2008) reported that the HWE of a mixture of southern hardwoods at 150 °C had a higher percent of hemicellulose than lignin. In their experiments, the WL at a 15 min extraction time was 3% (oven dry basis), 2% hemicellulose and 1% lignin. At 500 min there was a 26.4% WL, 19.7% hemicellulose, 3.6% lignin, and others. The most highly extracted hemicellulose was xylan, which increased as the extraction time was extended.

The properties of wood are highly dependent on their constituent polymers, cellulose, hemicellulose, and lignin. Thus, mechanical properties of the wood cell wall were quantified, specifically in the S2 layer of latewood cells, using nanoindentation. The results of the nanoindentation measurements are presented in Table 2.

For aspen, Meyer's hardness and modulus of elasticity (MOE) were significantly increased as SF increased until a SF of 3.56 was reached, after which continued increases in SF produced a reduction of both properties. With hemlock, however, SF

Table 2 Changes of hardness and MOE as a result of hot water treatment at different SFs

Treatment	Aspen		Hemlock	
	Hardness (MPa)	MOE (GPa)	Hardness (MPa)	MOE (GPa)
Control	403 ^a ± 30 ^{A,B}	13.6 ± 1 ^{A,B}	464 ± 22 ^{NS}	12 ± 1 ^A
SF 2.71	399 ± 48 ^A	12.2 ± 2 ^A	464 ± 21 ^{NS}	14 ± 1 ^B
SF 3.38	447 ± 59 ^{B,C}	15.5 ± 2 ^{B,C}	475 ± 17 ^{NS}	15 ± 2 ^B
SF 3.56	539 ± 44 ^C	17.4 ± 2 ^C	472 ± 30 ^{NS}	12 ± 2 ^A
SF 3.84	491 ± 47 ^C	15.9 ± 3 ^C	455 ± 32 ^{NS}	12 ± 3 ^A

These values were obtained using nanoindentation techniques from S2 layer of latewood (cell wall)

^a Mean is in mg/kg wood

^{A,B,C} Bonferroni multiple comparisons, at the 95.0% confidence level

^{NS} Not significant at 0.05 probability level

Table 3 Axial elastic modulus of wood strands, containing around 92% of earlywood, as a result of hot water treatment at different SFs

Treatment	Aspen			Hemlock		
	<i>D</i> (kg/m ³)	MC (%)	MOE (GPa)	<i>D</i> (kg/m ³)	MC (%)	MOE (GPa)
Control	403 ^a ± 22 ^{NS}	6.4 ± 0.9 ^A	5.0 ± 0.6 ^{B,C}	341 ± 23 ^{NS}	6.5 ± 1.0 ^A	3.0 ± 1.0 ^{NS}
SF 2.71	407 ± 22 ^{NS}	6.0 ± 0.9 ^{A,B}	6.0 ± 1.4 ^A	321 ± 28 ^{NS}	5.8 ± 1.1 ^{A,B}	2.8 ± 1.2 ^{NS}
SF 3.38	408 ± 44 ^{NS}	5.5 ± 1.1 ^{A,B}	4.9 ± 0.7 ^B	318 ± 60 ^{NS}	5.5 ± 1.4 ^{A,B}	2.9 ± 0.9 ^{NS}
SF 3.56	385 ± 39 ^{NS}	5.2 ± 0.6 ^{B,C}	5.0 ± 1.1 ^{B,C}	307 ± 40 ^{NS}	5.3 ± 1.1 ^{B,C}	2.8 ± 0.9 ^{NS}
SF 3.84	404 ± 41 ^{NS}	4.1 ± 0.5 ^C	3.0 ± 1.0 ^C	325 ± 54 ^{NS}	4.5 ± 0.9 ^C	2.9 ± 1.0 ^{NS}

Those results were obtained using DMA device

D density at test time, *MC* moisture content at test time

^a Mean is in mg/kg wood

^{A,B,C} Bonferroni multiple comparisons, at the 95.0% confidence level

^{NS} Not significant at 0.05 probability level

did not significantly affect hardness, while MOE significantly increased with SF until a SF of 3.38, after which increasing SF caused a reduction in this property.

The axial elastic modulus of mostly (92%) earlywood strands tested using DMTA is shown in Table 3.

Only aspen saw a statistically significant reduction at a SF of 3.84 while the control and the lower SFs were statistically homogenous groups. For hemlock there were no statistical differences in MOE among treatments. The flexural MOE for solid wood reported at 12% MC by the Forest Products Laboratory (1999) for aspen and hemlock is 9.9 and 8.3 GPa, respectively. These values approximate the average control MOE values reported in Tables 2 and 3 from nanoindentation and DMTA measurements. In both nanoindentation and DMTA test, an assumption was made that the samples had a similar MC as they had been conditioned together. Note, however, that the MC decreased with increasing SF, indicating lower equilibrium moisture content (EMC) conditions for extracted strands (Table 2).

While these differences in MC can influence the mechanical performance, this study found no significant effect of MC. As a summary, the mechanical performance increased the SF to 3.56, which accounts for a 22% overall increment. Beyond a SF of 3.56, the opposite effect occurs as a consequence of the hemicellulose extraction process.

Anatomical structural differences of wood also affect mechanical performance. The MOE derived from nanoindentation was higher than from DMTA due to the fact that the nanoindentation was done in the S2 layer of latewood while DMTA specimens consisted of primarily earlywood. According to Cramer et al. (2005), the differences in elastic properties between earlywood and latewood are due to the higher density, lower microfibril angle (MFA), and thicker cell wall of the latter. Larson et al. (2001) found that the density of earlywood is around 280 kg/m³ while latewood is about 600 kg/m³. In addition, Cramer et al. (2005) found that elastic properties of earlywood (EW) versus latewood (LW) varied by up to 2.7 (LW/EW). In this experiment, the ratio of LW/EW was 3.0 and 4.2 for aspen and hemlock, respectively (Cramer et al. 2005). However, Biblis (1969) found a ratio of LW/EW as high as 7 when studying variation in specific gravity and MOE among the earlywood and latewood.

As mentioned, much of the mechanical behavior of wood is governed by its polymers. Late and earlywood differ somewhat in their chemical compositions. In softwood, latewood contains more galactoglucomannans than earlywood, while earlywood has more xylans and lignin than latewood (Rowell 2005). However, in softwood the cellulose content in both regions is similar (Rowell 2005). Isolated glucomannan had a modulus around 2 GPa (dry) and 20 MPa (wet) (Salmen 2004). Cousins (1977) reported MOE values of isolated lignin between 4 and 7 GPa. The amorphous matrix of hemicellulose and lignin is embedded in cellulose, the latter being the contributor to the strength properties of wood. Theoretical estimations have concluded that the MOE of cellulose is 134–136 GPa (Salmen 2004). Other factors that govern the longitudinal elasticity of wood are cellulose content, the microfibril angle (MFA), and the degree of crystallinity of these cellulose microfibrils, all of which can vary considerably within a single tree or following wood modification (Gindl et al. 2004; Salmen 2004).

X-ray diffraction was used to investigate the change in the degree of crystallinity during the HWE process. Both species at initial stages of HWE showed an increase in the crystallinity up to a SF of 3.56. As extraction time was extended further, however, the degree of crystallinity began to decrease (Fig. 3).

There was a significant difference in crystallinity only for aspen ($p = 0.0076$) and hemlock ($p = 0.0490$), relative to the controls. According to studies on the effect of heat on wood and pure cellulose under moist and dry conditions done by Bhuiyan et al. (2000), wood cellulose has a higher crystallinity percentage than pure cellulose under both moist and dry conditions. The greatest increase in crystallinity in these studies was found when the wood cellulose samples were heated under moist conditions. The changes in crystallinity may be explained as crystallization in quasicrystalline or sub-crystalline structures due to rearrangement or reorientation of celluloses and hemicelluloses molecules, rather than loss of amorphous material (Howell et al. 2011).

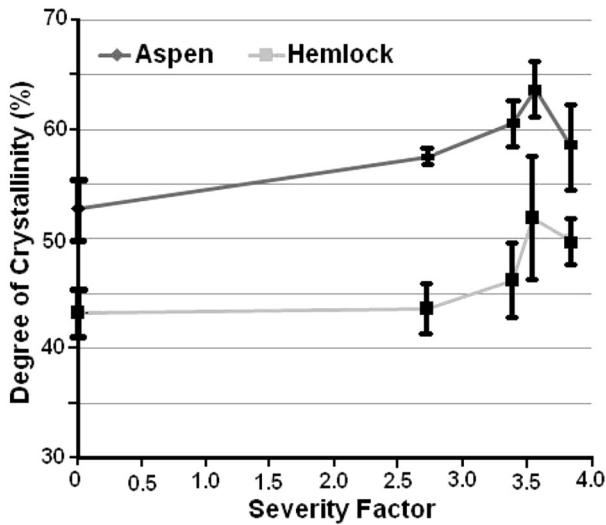


Fig. 3 Influence of hot water extraction on degree of crystallinity following different severity factor conditions

The properties of the cell wall are dominated by the S2 layer, since it is the thickest layer of cell wall and has higher cellulose content (58%) than the other layers (35%) (Fengel and Wegener 1984). The MFA has been shown to affect elastic properties (Gindl et al. 2004). It has also been found that subjecting wood to heat significantly increases the crystallinity (Bhuiyan et al. 2000). There is evidence that the change in crystallinity significantly influences the elasticity of wood (Gardner et al. 1993). Based on this, the degree of crystallinity versus MOE was plotted using the data obtained from the crystallinity and nanoindentation test. A weak correlation was found, determined by a second-order polynomial regression with a calculated coefficient of determination (R^2) of 0.634 for hemlock and 0.698 for aspen (Fig. 4).

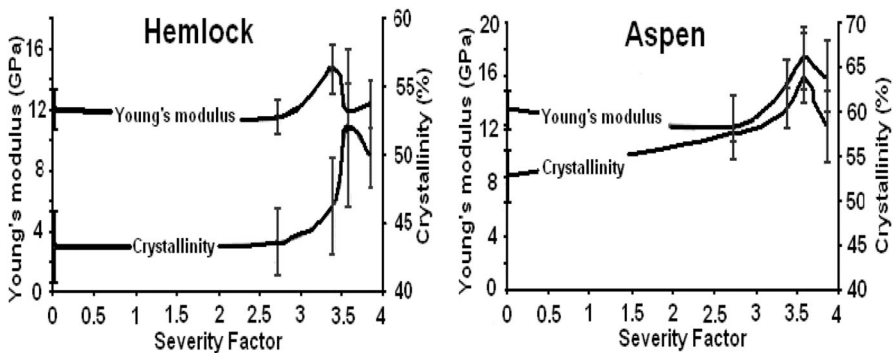


Fig. 4 MOE (nanoindentation) of the cell wall (S2 layer in latewood) as a function of degree of crystallization. The polynomial equation for the curve was adjusted using quadratic regressions, with a R^2 of 0.634 for hemlock and 0.698 for aspen

In conjunction with explaining the influence of HWE on MOE, it can be speculated that other factors, in improved crystallization through HWE, are affecting the elasticity of wood. Among these factors might be: (1) Micro-buckling of the wood associated with mass loss by HWE. This micro-buckling was evidenced when pore size and distribution of red maple (*Acer rubrum*) HWE strands were measured. It was found that the size of the cell wall pore structure increased by 22.2% after HWE, and scanning electron microscopy (SEM) showed that the number of pores in the cell wall increased as SF increased. (2) Changes in the degree of polymerization, along with other chemical and physical changes during HWE.

Conclusion

Understanding the mechanical properties of wood at different level and HWE conditions is important in developing high strength materials and added-value products. The general tendency was that aspen (hardwood) had greater WL than hemlock (softwood) at every SF. The elasticity of wood saw greater increases in the S2 layer of latewood than earlywood in both species. However, the MOE of aspen had a maximum 28% increase while the MOE of hemlock had a 22% increase at a SF of 3.56 and 3.38, respectively. An increase in percent crystallinity played an important role in the increase in mechanical properties of the cell wall, but it had a reduced correlation. Based on these data, it can be concluded that a WL between 10 and 13% is optimal for both woods, to maximize extraction and mechanical properties. As a result, to create a board with a target density more material is required compared to using regular wood. However, mechanical properties will observe a significant increase in the extracted strand boards thus resulting in greater resistance at the same density.

Acknowledgements Funding was provided by Universidad Tecnológica Centroamerica (UNITEC).

Open Access This article is distributed under the terms of the Creative Commons Attribution 4.0 International License (<http://creativecommons.org/licenses/by/4.0/>), which permits unrestricted use, distribution, and reproduction in any medium, provided you give appropriate credit to the original author(s) and the source, provide a link to the Creative Commons license, and indicate if changes were made.

References

- Bhuiyan MTR, Hirai N, Sobue N (2000) Changes of crystallinity of wood cellulose by heat treatment under dried and moisture conditions. *J Wood Sci* 46(6):431–436
- Biblis EJ (1969) Transition variation and relationships among properties within loblolly pine growth rings. *Wood Sci Technol* 3(1):14–24
- Borrega M, Karenlampi P (2008) Effect of relative humidity on thermal degradation of Norway spruce (*Picea abies*) wood. *J Wood Sci* 54(4):323–328
- Cousins WJ (1977) Elastic modulus of lignin as related to moisture content. *Wood Sci Technol* 10(2):9–17

- Cramer SM, Kretschmann DE, Lakes R, Schmidt T (2005) Earlywood and latewood elastic properties in loblolly pine. *Holzforschung* 59(5):531–538
- Fengel D, Wegener G (1984) *Wood: chemistry, ultrastructure, reaction*. Walter de Gruyter, Berlin
- Forest Product Laboratory (1999) *Wood handbook—wood as an engineering material*. General technical report FPL-GTR-113. U.S. Department of Agriculture, Forest Service, Forest Product Laboratory, Madison, WI
- Gardner DJ, Gunnells DW, Wolcott MP, Amos L (1993) Changes in wood polymers during the pressing of wood composites. In: Kennedy JF, Phillips GO, Williams PA (eds) *Cellulosics, chemical, biochemical and material aspects*. Ellis Horwood, New York, pp 513–518
- Gindl W, Gupta HS, Schöberl T, Lichtenegger HC, Fratzl P (2004) Mechanical properties of spruce wood cell walls by nanoindentation. *Appl Phys A* 79(8):2069–2073
- Hill C (2006) *Wood modification: chemical, thermal, and other processes*. Wiley, Hoboken
- Howell C, Hastrup A, Goodell B, Jellison J (2009) Temporal changes in wood crystalline cellulose during degradation by brown rot fungi. *Int Biodeterior Biodegrad* 63:414–419
- Howell C, Hastrup A, Jara R, Larsen F, Goodell B, Jellison J (2011) Changes in wood crystalline cellulose structure caused by hot-water extraction and brown-rot decay. *Cellulose* 18:1179–1190
- Jakes JE, Frihart CR, Beecher JF, Moon RJ, Stone DS (2008) Experimental method to account for structural compliance in nanoindentation measurements. *J Mater Res* 23(4):1113–1127
- Jakes JE, Frihart CR, Beecher JF, Moon RJ, Resto PJ, Melgarejo ZH, Suárez OM, Baumgart H, Elmustafa AA, Stone DS (2009) Nanoindentation near the edge. *J Mater Res* 24(3):1016–1031
- Konnerth J, Gindl W (2006) Mechanical characterization of wood-adhesive interphase cell wall by nanoindentation. *Holzforschung* 60(4):429–433
- Larson PR, Kretschmann DE, Clark III A, Isebrands JG (2001) *Formation and properties of juvenile wood in southern pine*. General technical report FPL-GTR-129. U.S. Department of Agriculture, Forest Service, Forest Product Laboratory, Madison, WI
- Mosier N, Ladisch C, Ladisch M (2002) Characterization of acid catalytic domains for cellulose hydrolysis and glucose degradation. *Biotechnol Bioeng* 79(6):610–618
- Nishiyama Y, Langan P, Chanzy H (2002) Crystal structure and hydrogen-bonding system in cellulose I β from synchrotron X-ray and neutron fiber diffraction. *J Am Chem Soc* 124(31):9074–9082
- Oliver WC, Pharr GM (2004) Measurement of hardness and elastic modulus by instrumented indentation: advances in understanding and refinements to methodology. *J Mater Res* 19(1):3–20
- Overend RP, Chornet E (1987) Fractionation of lignocellulosic by steam-aqueous pretreatments. *Philos Trans R Soc A* 321(1561):523–536
- Ramiah MV, Goring DAI (1967) Some dilatometric measurements of the thermal decomposition of cellulose, hemicellulose and lignin. *Cell Chem Technol* 1(3):277–285
- Rietveld HM (1967) Line profiles of neutron powder-diffraction peaks for structure refinement. *Acta Crystallogr* 22(1):151–152
- Rietveld HM (1969) A profile refinement method for nuclear and magnetic structures. *J Appl Crystallogr* 2(2):65–71
- Rowell RM (2005) *Handbook of wood chemistry and wood composites*. CRC Press, London
- Rusche H (1973) Thermal degradation of wood at temperatures up to 200 °C. I. Strength properties of wood after heat treatment. *Holz Roh Werkst* 31(7):273–281
- Salmen L (2004) Micromechanical understanding of the cell-wall structure. *Comptes Rendus Biol* 327(9–10):873–880
- Sattler C, Labbé N, Harper D, Elder T, Rials T (2008) Effects of hot water extraction on physical and chemical characteristics of oriented strand board (OSB) wood flakes. *Clean Soil Air Water* 36(8):674–681
- Sjöström E (1993) *Wood chemistry: fundamentals and applications*, 2nd edn. Laboratory of Wood Chemistry, Forest Products Department, Helsinki University of Technology, Espoo
- Tunc M, van Heiningen ARP (2008) Hemicellulose extraction of mixed southern hardwood with water at 150 °C: effect of time. *Ind Eng Chem Res* 47(18):7031–7037
- Tze WTY, Wang S, Rials TG, Pharr GM, Kelley SS (2007) Nanoindentation of wood cell walls: continuous stiffness and hardness measurements. *Compos Part A Appl Sci* 38(3):945–953
- Wimmer R, Lucas BN (1997) Comparing mechanical properties of secondary wall and cell corner middle lamella in spruce wood. *Iawa J* 18(1):77–88
- Wimmer R, Lucas BN, Tsiu TY, Oliver WC (1997) Longitudinal hardness and Young's modulus of spruce tracheid secondary walls using nanoindentation technique. *Wood Sci Technol* 31(2):131–141